CONCRETE DETERIORATION FROM PYRITE STAINING, SEWER GASES, AND CHIMNEY FLUE GASES – CASE STUDIES SHOWING MICROSTRUCTURAL SIMILARITIES

Dipayan Jana

Applied Petrographic Services, Inc., and Construction Materials Consultants, Inc. Greensburg, PA, USA

ABSTRACT

Case studies are presented to show chemical deterioration of concrete exposed to three different moist, oxidizing environments, where oxidation generated sulfuric acid, which, in turn, has caused acidic corrosion and associated sulfate attacks in concrete. Concrete containing unsound pyrite inclusions in the near-surface aggregate particles commonly show staining and popout, and associated sulfuric acid-induced decomposition of paste around the unsound particles. Concrete liners in chimney environments often show acidic corrosion of the inner wall of liner, carbonation, and white calcium sulfate deposits, from interactions of moist sulfur and carbon dioxide flue gases with the portland cement hydration products. Concrete sewer channels show similar acidic corrosion of the inner wall, mostly in the aerated portion, due to oxidation of sewer gases (hydrogen sulfide) by aerobic bacteria that colonizes on the moist aerated portions. Although the attacks in present cases are primarily of sulfuric acids, the products of such attacks, i.e., gypsum, can cause concomitant sulfate attacks, with microcracking and further decomposition of paste. Corrosion, microcracking, staining, discoloration, leaching and decomposition of portland cement hydration products, carbonation, and gypsum formation in cracks and voids are some common microstructural features that develop from these combined acidic and sulfate attacks, which are similar to the ones observed in many classical external sulfate attacks in concrete from exposure to a sulfate-rich soil. Case studies show the importance of detailed petrographic examinations in evaluating condition of concrete in such environments, depths of attacks, and anticipated future durability.

INTRODUCTION

Chemical deterioration of a portland cement concrete is often accompanied by decomposition of portland cement hydration products by chemical agents, either from the external environment where the concrete is exposed, or, from internal ingredients of concrete. Examples of pathways of such deterioration include ingress of acidic or sulfate solutions into concrete, such as from the acidic soil or sulfate-rich ground where a concrete structure is exposed. Acid or sulfate attacks commonly cause leaching, carbonation, softening of paste, precipitation of innocuous or potentially deleterious (e.g., expansive) secondary deposits, with concomitant loss of mass, strength, and, in ultimate cases, serviceability of concrete. In many cases, concrete surfaces exposed to such solutions show progressive scaling (i.e., loss of the exposed surface) and cracking at different degrees, which open up channels for further ingress of chemicals, and continued attacks. Depth of deterioration often depends on concentrations of chemicals in the solutions, types of chemicals, static or migratory nature of chemicals, moisture conditions, and the type and quality of concrete exposed to such environment.

The present paper discusses case studies of three such attacks – in widely different environments (see Figure 1) – all involving ingress of acidic/sulfate solutions, originating either from agents present in concrete ingredients, or from the external environments to which the concrete is exposed. In all cases, such attacks represent a secondary mechanism of concrete deterioration, i.e., occurred in association with other primary mechanisms, which have caused the major (i.e., visible) deterioration in concrete. The study shows similarities in the microstructures of deteriorated concretes from such different environments due to the similarities in the mechanisms of acid/sulfate attacks.

In the first case study, fine broom-finished surface of concrete sidewalks and walkways show extensive occurrences of isolated, small-scale unsightly reddish brown stains and popouts from unsound pyrite (FeS_2) inclusions in the coarse aggregate. The unsound particles, situated at or near (i.e., within the top ½ in.) the finished surface show softening, fracturing, popout and staining of concrete above the particle, and microcracking in concrete around the particles – all from expansive stresses associated with pyrite oxidation, which is the primary mechanism of concrete surface distress. Paste surrounding the unsound pyrite, however, show softening, microcracking, and secondary chemical deterioration from sulfuric acid, generated as a byproduct of pyrite oxidation in a moist environment.

The second case study shows concrete deterioration in a chimney environment, where sulfur-rich flue gases (SO_2 and CO_2) have generated sulfuric acid in a moist environment, and caused acid and sulfate attacks on the exposed concrete liner wall in the chimney. The presence of alkali-silica reactive aggregate particles, along with intermittent moist exposure, and the high alkali-cement used in this old (pre-1950s) concrete chimney have caused cracking due to deleterious alkali-silica reactions. High temperatures of the chimney have caused discoloration and some thermal cracking of concrete along the inside wall, due to differential thermal expansions of aggregates and paste. Besides these primary mechanisms of concrete deterioration, the inside wall of the concrete liner shows chemical decomposition of paste from sulfuric acids generated from oxidized flue gases in a moist environment.

The third case study is from a concrete pipeline in a sewer environment, where hydrogen sulfide gas generated inside the moist sewer environment has been oxidized to sulfuric acid, and caused acid and sulfate attacks on the concrete lining. In this study, portions of concrete liner continuously submerged under sewage effluent show minimal deterioration, whereas portions intermittently exposed to moist air above sewage show severe deterioration.

Gypsum is the common secondary deposit in all three environments, formed as a result of reactions of sulfuric acid with portland cement hydration products (calcium hydroxide and calcium silicate hydrate), sulfate attack, and associated decomposition of paste.

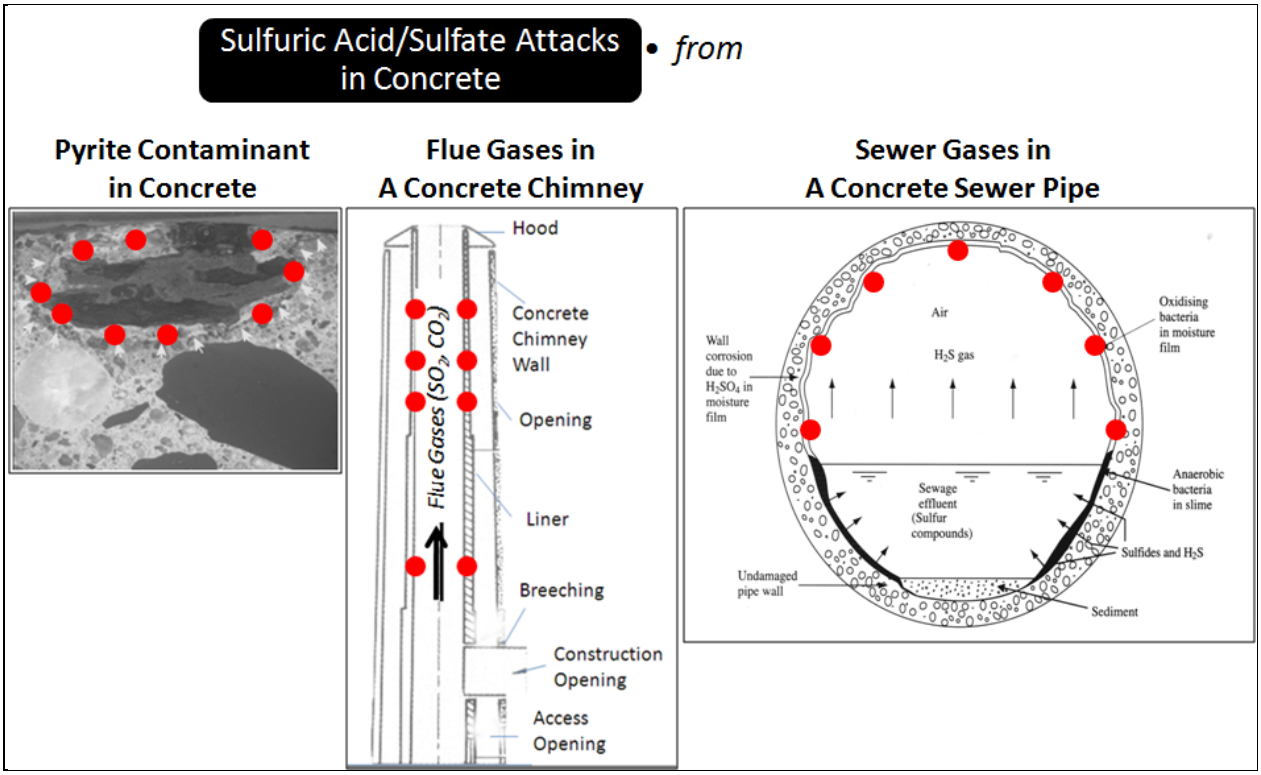

Figure 1 – Sulfuric acid and sulfate attacks in concrete in three different environments (red dots show locations of concrete deterioration) [1,2].

METHODS OF LABORATORY STUDIES

The samples were examined by detailed petrographic examinations, *a la* ASTM C 856 "Standard Practice for Petrographic Examination of Hardened Concrete." Methods used are: (a) detailed visual examinations of samples, as received, (b) observations of as received, fresh fractured, finely ground (lapped), and thin sections of samples by using a low-power stereo microscope, (c) examinations of oil immersion mounts and thin sections of samples in a petrographic microscope (having reflected, transmitted, and fluorescent-light facilities), (d) digital photomicrography of lapped and thin sections by using high-resolution digital cameras attached to optical microscopes and image capture and analysis software, (e) x-ray diffraction analyses of deteriorated products, (f) scanning electron microscopy (backscatter and secondary electron imaging) of microstructure of deteriorated concrete, (g) associated energy-dispersive x-ray microanalyses of the products of concrete deteriorations, and (h) elemental mapping of concrete microstructure around the deteriorated portions.

Since the samples of these case studies often contained fragile, softened, and highly decomposed surfaces that were directly in contact with the aggressive agents, careful and appropriate preparation of samples preserving the pristine deteriorated microstructure, for petrographic examinations, was of utmost importance. Samples were usually treated as follows: (a) samples were first photographed, all sides, as received; (b) described in detail; (c) then carefully sectioned (longitudinally) by using thin water-cooled continuous rim diamond saws; (d) sectioned surfaces were sometimes oven-dried and vacuum impregnated with low-viscosity epoxy resin (to improve the integrity of softened and decomposed surfaces); (e) surfaces thus prepared were then ground to smooth, flat, deformation-free, almost light-reflective surfaces by carefully grinding on progressively finer-sized metal-bonded diamond discs magnetically attached to a horizontal rotary iron lapping wheel; (f) remaining portions of sectioned surfaces were trimmed to small blocks (keeping particular attention to the surfaces exposed to deleterious agents), oven-dried, vacuum-impregnated with low-viscosity dyed-epoxy, and used for preparation of large-area (2 × 3 in.) thin sections (~ 30-micron thickness); (g) the prepared thin sections, and residual blocks from thin section preparations were polished for SEM-EDS studies; and finally, (h) to determine the mineralogical compositions, products of concrete deterioration were sometimes ground to fine powders (< 10 micron size) for x-ray diffraction analysis.

Samples were examined and analyzed by using Nikon SMZ-10A and Olympus SZH12 stereomicroscopes at 10 to 100x magnifications, Nikon Labophot 2 POL and Olympus BX-40 petrographic microscopes at 40 to 1000x magnifications, CamScan Series II scanning electron microscope at 10 to 50,000x magnifications with accelerating voltages from 10 to 20KV, Siemens D5000 x-ray Diffractometer with Cu-Kα radiation, and Epson 4800dpi flatbed scanner. Optical microscopical images were captured by using several high-resolution digital cameras and edited with image analysis software.

CASE STUDY I: CONCRETE SURFACE STAINING FROM PYRITE INCLUSIONS

Background – Concrete sidewalks, stairs, and driveways in a residential complex showed unsightly stains (see Figure 2) all over the complex, within a year of placement. Stains occurred on fine broom-finished surface of a 4-in. thick concrete slab-on-grade. Individual stains often created popout, and fractured remains of dark gray to black, $^1/_8$ to $^1/_2$ in. size aggregate at the center of small, micro-crater type depressions (less than $^1/_2$ in. size), at the location of maximum intensity of stain. The stains occur as typical comet-tail type pattern having the origin of stain at and around the near-surface, popout-forming, unsound aggregate particles, and an elongated tail of progressively lesser intensity of reddish brown tone laterally spread out as a comet tail, with an overall extension of 3 to 6 in. The stain trails also show darker reddish brown tone towards the central portion of the trail, which fades out to lighter yellowish brown color towards the tail edges.

Concrete – Three concrete cores were received from over three isolated stains on a sidewalk, driveway, and stairway. The concrete in all three cores is determined to be similar, made using the same concrete mix. The concrete is air entrained and made using crushed limestone coarse aggregate having a nominal maximum sizes of 3/4 in., natural siliceous sand fine aggregate having a nominal maximum size of 1/4 in., a cementitious materials content estimated to be equivalent to 6 1/2 to 7 bags of portland cement per cubic yard, of which 20 to 25 percent is estimated to be ground granulated blast furnace slag, and a water-cementitious materials ratio uniform within and between the cores, and estimated to be from 0.48 to 0.52. The concrete is dense and well consolidated. The air content is estimated to be 3 to 4 percent at the top 1/4 in. and 5 to 6 percent in the body. The concrete has a good air-void system, which is consistent with the industry-recommended air void parameters for an air-entrained concrete to be durable in a cyclic freezing and thawing environment. There is no evidence of inadequate curing or finishing-related improprieties found in the cores. The concrete shows normal nominal atmospheric carbonation to a depth of 1/8 in. from the broom-finished surface.

Source of Stain-Producing Particles – The coarse and fine aggregate particles are well graded and well distributed. The natural sand fine aggregate particles contain major amounts of quartz, minor amounts of quartzite, and trace amounts of chert and mafic minerals; particles have been sound during their service in the concrete.

A minor portion of coarse aggregate, constituting dark pyrite grains, however, showed unsoundness as popouts and surface staining. Except for the pyrite grains, however, the majority of the crushed limestone coarse aggregate particles contains calcitic limestone, carbonate mudstone, siliceous limestone, and argillaceous limestone, which have been sound during their service in the concrete.

Many argillaceous limestone particles contain negligible amounts of very fine pyritic inclusions in the carbonate matrix, which appeared to be present in sound condition. It is the separate dark gray to black, angular, pyrite and oxidized pyrite grains, from 1/8 to 1/2 in. size, probably came from pyrite-bearing veins or strata in the argillaceous limestone formation from where the aggregate was quarried, which is present as a potentially unsound, deleterious 'contaminant' in the crushed limestone aggregate. Particles situated near the surface during concrete placement and finishing showed popout and surface staining; particles deeply buried inside the body did not show staining. There is no evidence of alkali-aggregate reactions of coarse or fine aggregate particles in the concrete.

The total amount of potentially stain-producing unsound pyrite grains in the body of the concrete is estimated to be very low, e.g., less than 2 percent by volume of coarse aggregate. Despite the low amount, however, there were enough particles, situated immediately beneath the finished surface that have caused widespread occurrence of staining, noticeable enough to warrant this investigation.

It is, however, important to mention that even with noticeable frequency of stains on the surface and lateral extension of individual stains on the surface, in each area of stain, the extent of "internal deterioration" of concrete by the stain-producing particle is very localized, e.g., up to a maximum vertical cross-sectional area of 1/4 in. deep × 1/2 in. lateral extension in the three cores examined (the size of the affected area depends on the size of the pyrite particle).

Concrete beneath the surface region (i.e., beyond 1/4 to 1/2 in. depth) was present in sound condition. Despite the presence of pyrite all throughout the depth of the cores, restricted supply of oxygen and moisture in the interior concrete, necessary for pyrite oxidation, has restricted the distress only at and near the finished surface. Therefore, a prior understating of their presence in the coarse aggregate, their potential to cause surface stain, and, as a consequence, a deep embedding of those unsound particles during concrete placement and finishing could have reduced the occurrence of surface staining.

Surface Stains on Cores – Each core contained: (a) a dark reddish brown stain on an otherwise sound, fine broom-finished surface (Figure 2); and (b) a fractured remain of a dark gray to black, 1/8 in. to 1/2 in. size aggregate particle at the center of a small, shallow, micro crater-type hole on the surface (less than 1/2 in. size) where the stain has the maximum intensity and the unsound aggregate particle has caused popout.

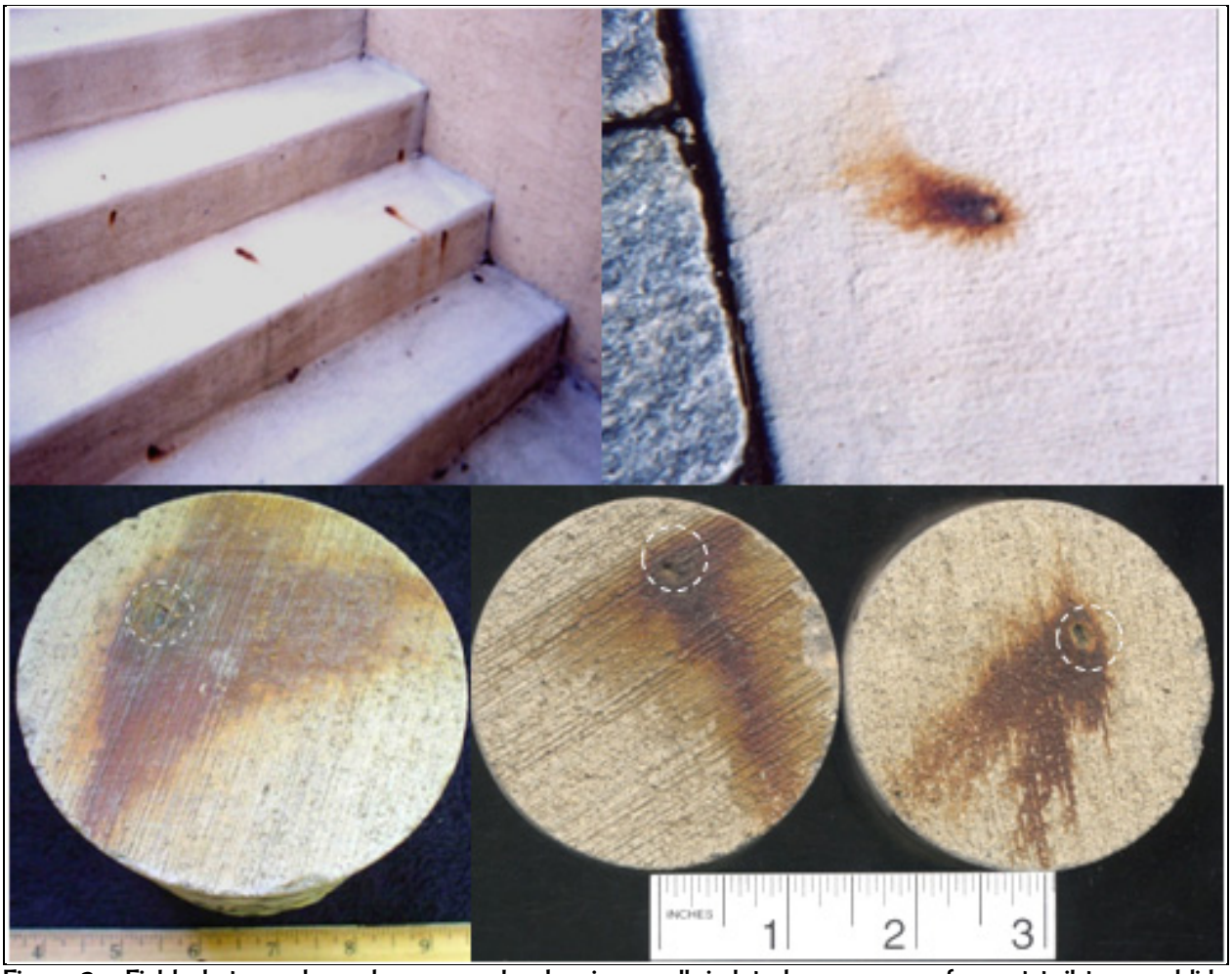

Figure 2 - Field photographs and core samples showing small, isolated occurrences of comet-tail type reddish brown stains on concrete surface from oxidation of near-surface pyrite inclusions in crushed limestone coarse aggregate. In most cases, as seen in three cores, maximum staining occurred at and around the oxidized pyrite grain (marked with dashed circles), many of which have caused small surface popouts, with progressively decreasing degree of stain away from the unsound particle as a comet-tail pattern.

Based on the direct association of the popout-forming, fractured, near-surface, unsound aggregate particles with the stains, and the maximum intensity of the stain at and immediately around the particles, the surface staining is judged to have originated from the popout-forming, unsound aggregate particles. Based on the examinations of field photos and core top surfaces, staining and aggregate popout-formation are, therefore, judged related to each other.

Based on detailed petrographic examinations, surface staining is determined to be due to atmospheric oxidation of near-surface pyrite inclusions in coarse aggregate, in the presence of oxygen and moisture from the atmosphere and alkaline pore solutions in concrete. The unsound particles occur as isolated grains, similar in size fractions of the coarse aggregate (from $^1/_8$ to $^1/_2$ in. size) and not as inclusions within the limestone particles (although argillaceous limestone particles also contain pyrite inclusions but did not cause surface staining).

Microstructure – A detailed examination of the internal microstructure of a surface stain, sectioned through the stain producing pyrite grain shows the following characteristic microstructure (the following discussion involves a vertical cross sectional area of $^1/_4$ in. deep by $^1/_2$ in. lateral distance through an unsound particle, shown in the vertical cross sections below):

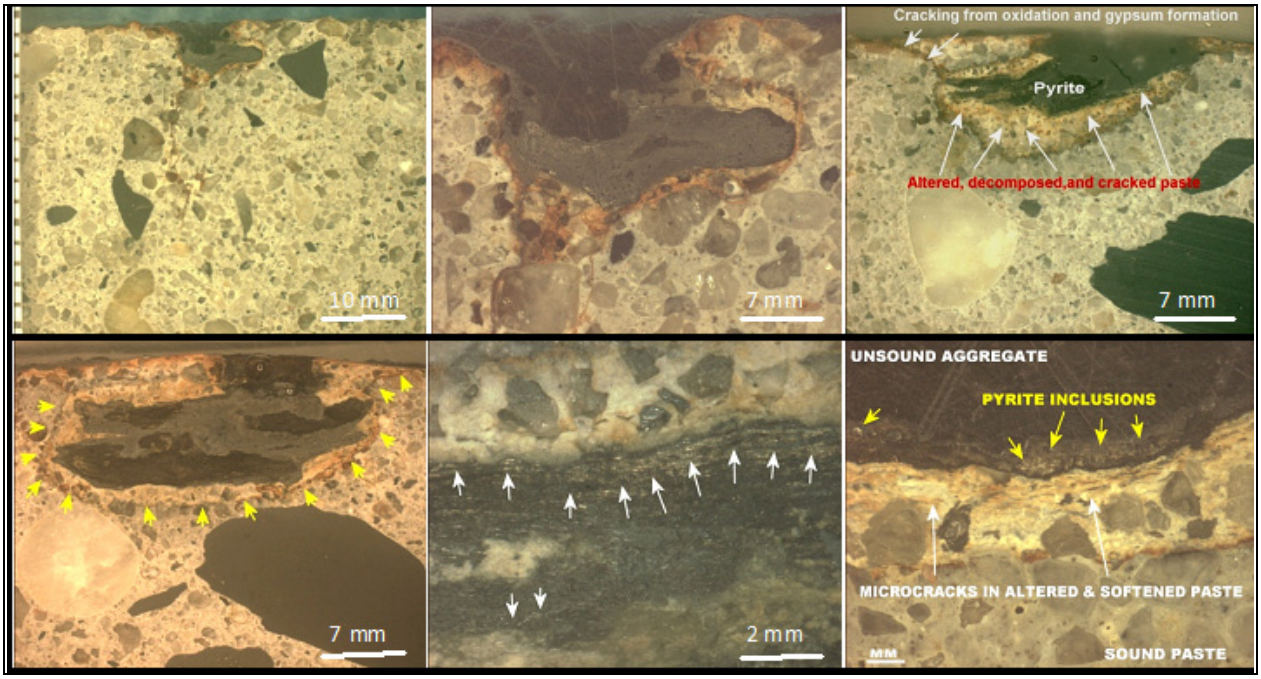

Figure 3 - Photomicrographs of lapped cross sections of concrete cores showing oxidized pyrite grain, light brown decomposed paste immediately adjacent to the oxidized pyrite, which is surrounded by a thin reddish brown oxidation rim; residual golden yellow pyrite in the black oxidized mass, and microcracking in concrete associated with pyrite oxidation.

(a) The Ring Structure – The interior of a stain shows a typical ring-structure (Figure 3), consisting of a central, dark oxidized pyrite grain, which is surrounded by a thin, narrow band of light brown colored, severely altered, micro cracked, carbonated, and decomposed paste, which, in turn, is surrounded by and separated from the outside unaltered, or less altered, uncracked paste by a thin reddish brown oxidation rim.

(b) The Oxidized Pyrite Grain – Severe atmospheric oxidation has changed the typical golden yellow color of the original pyrite grains to dark gray to black, variably porous and softened oxidized mass. A few remains of the original golden yellow pyrite are still observed as disseminated, discontinuous bands within the oxidized particle (Figure 3). The grain shows severe microcracking due to the expansion associated with oxidation, and the resultant popout. Microcracking is more severe towards the periphery of the particle than that at the interior; and many cracks contain gypsum as secondary deposits. The overall cross section of a grain shows a banded nature (Figure 4) with alternating bands of iron sulfate (Areas 1 and 3 in Figure 4, top right photo) and iron-potassium-sulfate (Area 2 in Figure 4, top right photo).

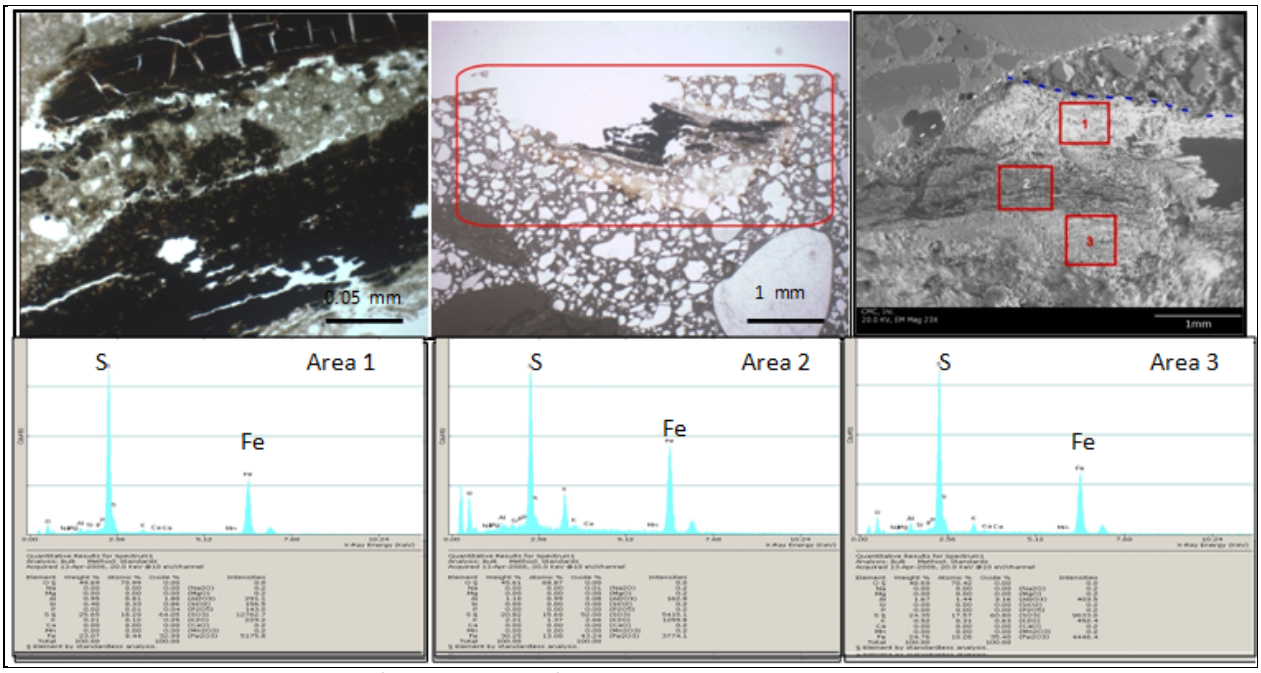

Figure 4 - Photomicrographs of thin sections of concrete cores showing dark, isotropic oxidized pyrite grain, which has caused popout and microcracking (top left and middle photos). The top right photo shows backscatter electron image of an oxidized pyrite (within dashed lines), which has been severely deteriorated and shows an alternating light and dark color banded structure. Areas marked as 1, 2, and 3 from the alternating bands were analyzed by energy-dispersive x-ray microanalysis (EDS) and shown in the bottom left, middle, and right spectrum, respectively. All three spectra show broad compositional similarities between the bands in pyrite containing iron and sulfur as the principal elements. The oxygen peaks in these spectra indicate the presence of iron oxide/hydroxide products (higher oxygen in the darker band, Area 2).

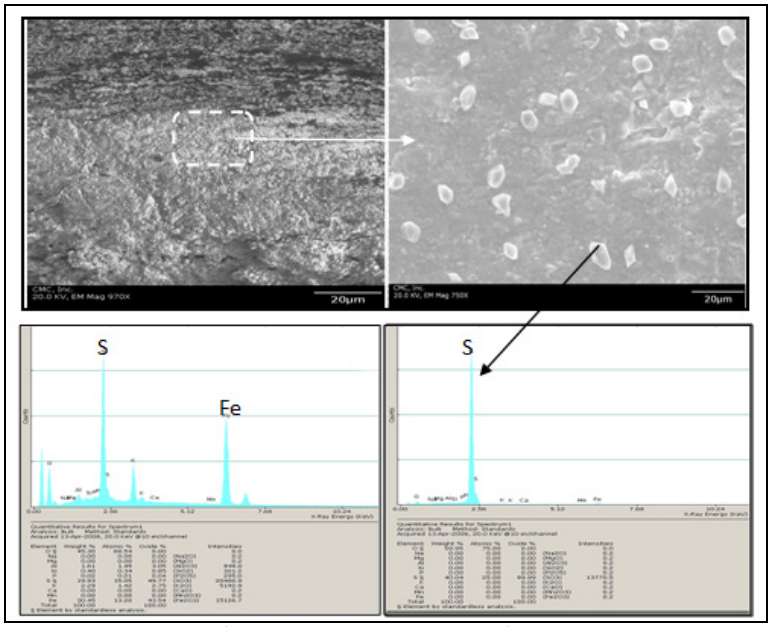

Figure 5 - Backscatter electron image of the banded structure of oxidized pyrite, where the relatively lighter band shows very fine, isolated grains of elemental sulfur. The bottom left EDS spectrum of the overall light band, containing predominantly iron and sulfur; the right spectrum is of the small grains of elemental sulfur (as shown in the top right photo) within the oxidized mass. Notice the presence of oxygen peak in the left spectrum (indicating the presence of iron oxide/hydroxide), and its absence in the right spectrum of individual small grains.

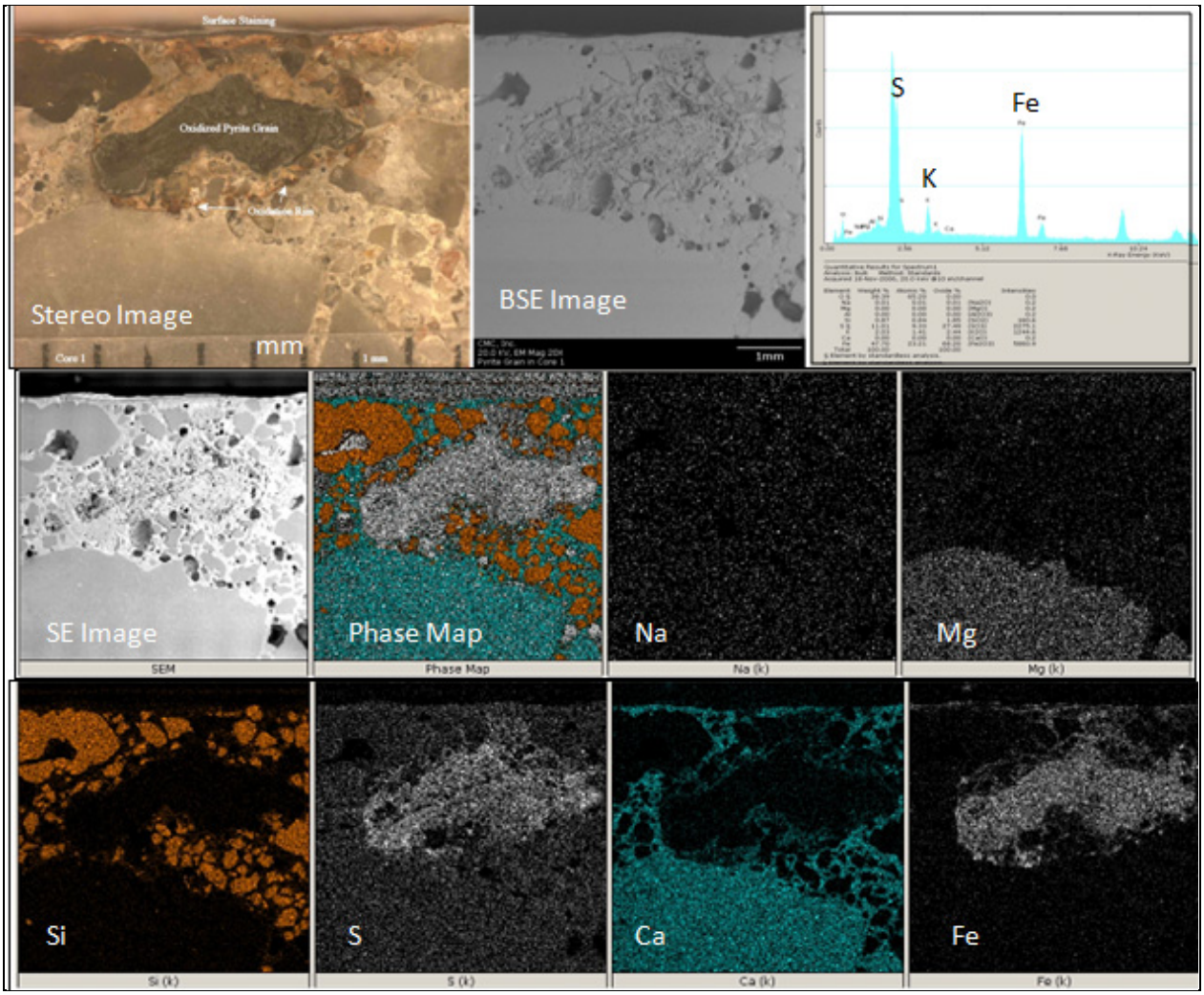

Figure 6 - Photomicrographs of lapped cross section of a concrete core (top left photo), backscatter electron image (top middle photo), and x-ray elemental analysis of another oxidized pyrite grain situated immediately beneath the stained surface. The bottom photos show x-ray elemental maps of oxidized pyrite and surrounding area in concrete, where the oxidized pyrite grain is highlighted by iron and sulfur maps.

(c) <u>The Altered, Decomposed, and Microcracked paste</u> – Immediately adjacent to the oxidized pyrite grain is a narrow band of severely altered, decomposed, carbonated, and softened light brown paste (Figures 3 and 7), from less than 1 mm to 3 mm in cross sectional thickness, containing several parallel microcracks (oriented parallel to the margin of the oxidized pyrite grain) that are often filled with gypsum (Figures 7 and 8). Some cracks are radial in nature and have extended from the altered paste into the neighboring less altered or sound paste region situated outside the ring structure (Figure 7). Some radial cracks originated from the oxidized pyrite grain and extended through the altered paste band into the sound paste region. The air voids within the altered paste band are often filled or lined with secondary gypsum deposits.

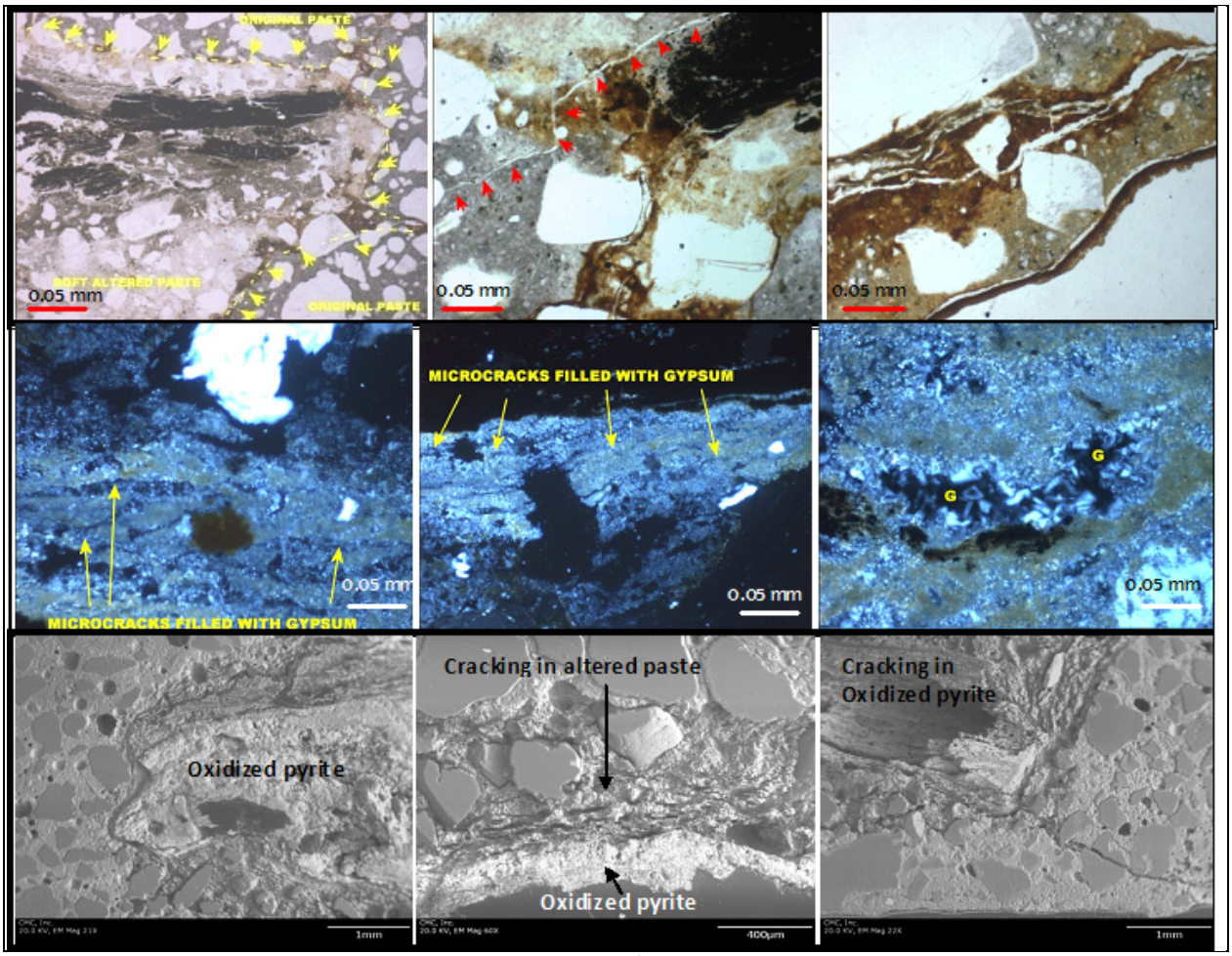

Figure 7 – Top Row = Thin section photomicrographs of concrete core showing the dark, isotropic, cracked, oxidized pyrite, altered and decomposed paste immediately adjacent to the oxidized pyrite, reddish brown oxidation stain invading the paste adjacent to the pyrite, and microcracking in paste from pyrite oxidation.

Middle Row = Thin section photomicrographs (in crossed-polarized light) showing severe microcracking, carbonation, softening, and decomposition of paste immediately adjacent to the oxidized pyrite and gypsum deposits in microcracks and in voids in the altered paste. The sample was impregnated with a blue dye-mixed epoxy to improve its integrity at the surface region and highlight these microcracks.

Bottom Row = Backscatter electron images showing severe microcracking in pyrite and in the altered paste adjacent to the oxidized pyrite grain.

(d) <u>The Reddish Brown Oxidation Rim Around the Altered Paste</u> – A thin, dark reddish brown oxidation rim defines the periphery of the ring structure and separates the altered paste from the outer unaltered or less altered bulk paste region of the concrete (Figures 3 and 7). The margin of the oxidation rim more or less follows the corresponding periphery of the central oxidized pyrite grain, from where ferruginous elements of the rim have originated, and migrated through the decomposed paste to form the rim. Formation of iron hydroxide (goethite), as determined in the x-ray diffraction pattern of oxidized pyrite in Figure 9, is responsible for the reddish brown oxidation rim.

(e) <u>The Outer Sound or Less Altered Paste</u> – Paste outside the ring structure is significantly denser and harder than the altered paste within the ring and does not contain any microcracks, except for the ones originated within the ring and extended out. Air voids in the outer paste situated immediately adjacent to the ring structure contain gypsum crystals (Figure 8, similar to the ones found in voids within the ring in Figure 7) and indicates migration of sulfate solutions outside the ring and crystallization of secondary gypsum in the voids situated adjacent to the ring. Secondary gypsum crystallization in air voids in the sound region outside the ring is detected down to a depth of 1 in. There is a systematic decrease in the amount of secondary gypsum crystals in air void walls in the sound paste. Voids situated further away from the ring contain both gypsum and fine acicular secondary ettringite crystals.

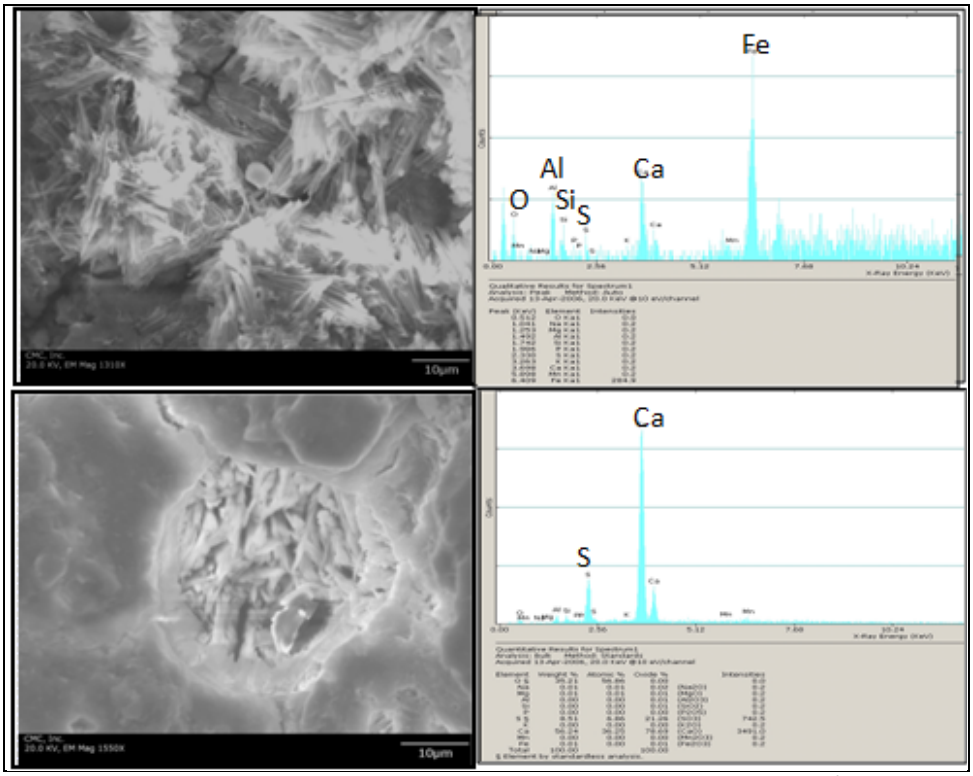

Figure 8 - Secondary electron images and associated EDS spectrum of secondary deposits in voids adjacent to the altered paste around oxidized pyrite; the top photo shows the presence of gypsum, iron oxide, and carbonated products of paste (EDS spectrum shows peaks for Fe, Ca, Al, S, and Si); the bottom photo and the spectrum show the gypsum deposits in a void (EDS spectrum shows peaks for Ca and S).

Similar ring structure and associated characteristic microstructure is found in all three cores around their popout-forming and stain-producing near-surface oxidized pyrite grains.

Several other case studies of surface staining by pyrite oxidation and popout showed very similar microstructure of oxidized pyrite, decomposed paste and oxidation rim, with associated gypsum deposits in voids and microcracks.

X-ray Diffraction Analysis of a Near-Surface Pyrite Grain – Polished cross section of a concrete sample containing a near-surface oxidized pyrite grain was placed on Siemens D 5000 X-ray Diffractometer and scanned at a slow rate (1°/min) with Cu-Kα radiation at 30nA-40kV current-voltage conditions. The result shows the presence of a minor amount of residual pyrite in a goethite mass in the grain (the main peaks of quartz are from the associated sand in concrete around the pyrite grain).

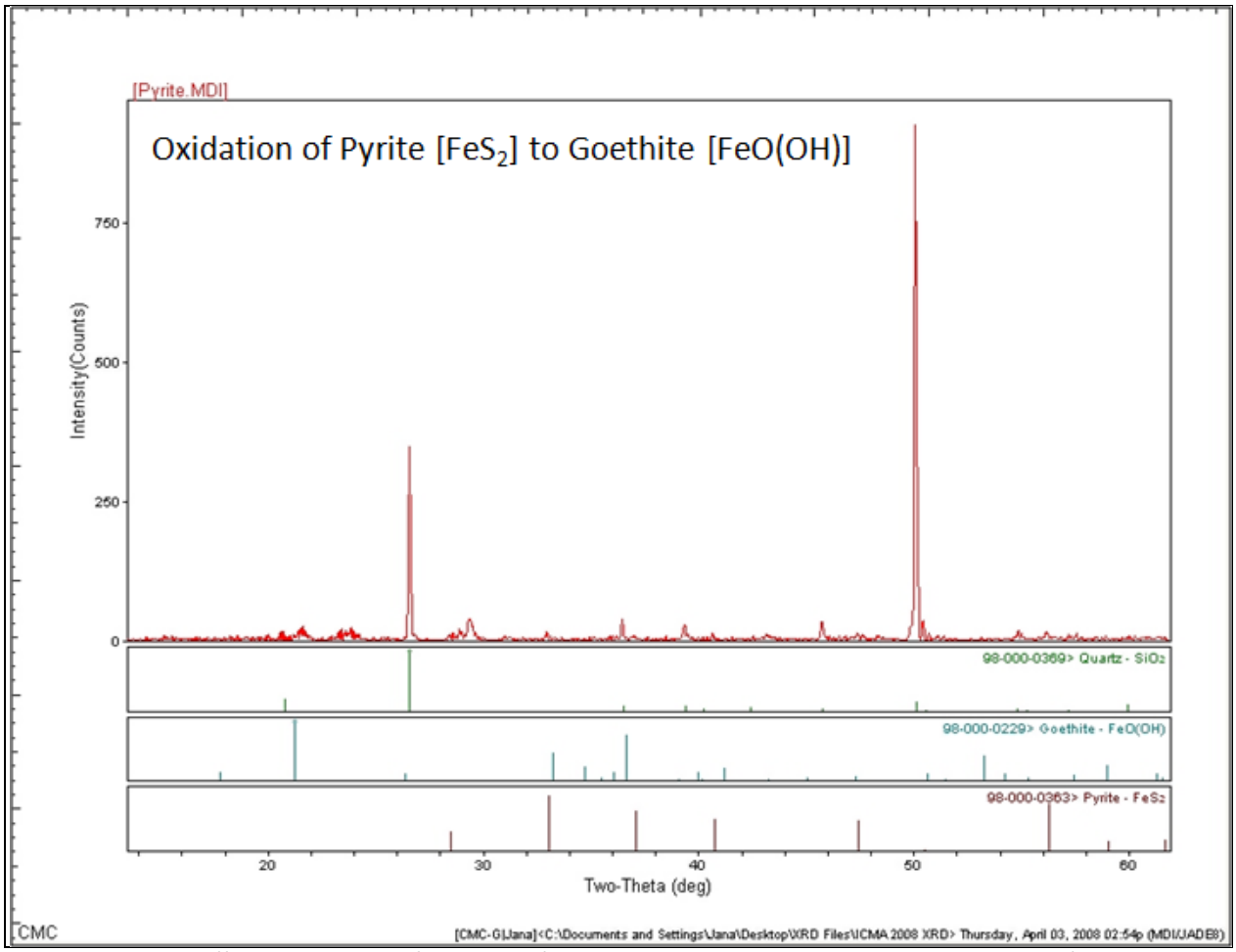

Figure 9 – X-ray diffraction pattern of a near-surface oxidized pyrite grain showing the presence of goethite, the oxidation product of pyrite, along with residual pyrite and abundant quartz from nearby sand aggregate.

Mechanism of Pyrite Staining – In the presence of atmospheric moisture, oxygen, and alkaline pore solution of concrete, the near-surface pyrite grains have oxidized to iron sulfate and sulfuric acid [1, Figure 10]; the former has further oxidized to iron oxide and hydroxide (ferrous to ferric hydroxide or goethite, which causes the stain), and, the latter has softened and decomposed the paste and produced gypsum in carbonated regions. Oxidation of iron sulfide (pyrite) to iron oxide (goethite) through iron sulfate, and, gypsum formation in the paste from sulfuric acid attack are both expansive reactions, which have caused expansion and popout of the unsound particles and associated microcracking in the particle and in surrounding paste (both parallel cracking in the altered paste zone around the particle and radial cracking from the particle into the paste). The following diagram describes the mechanism of staining and gypsum formation by oxidation of pyrite contaminants in concrete aggregates:

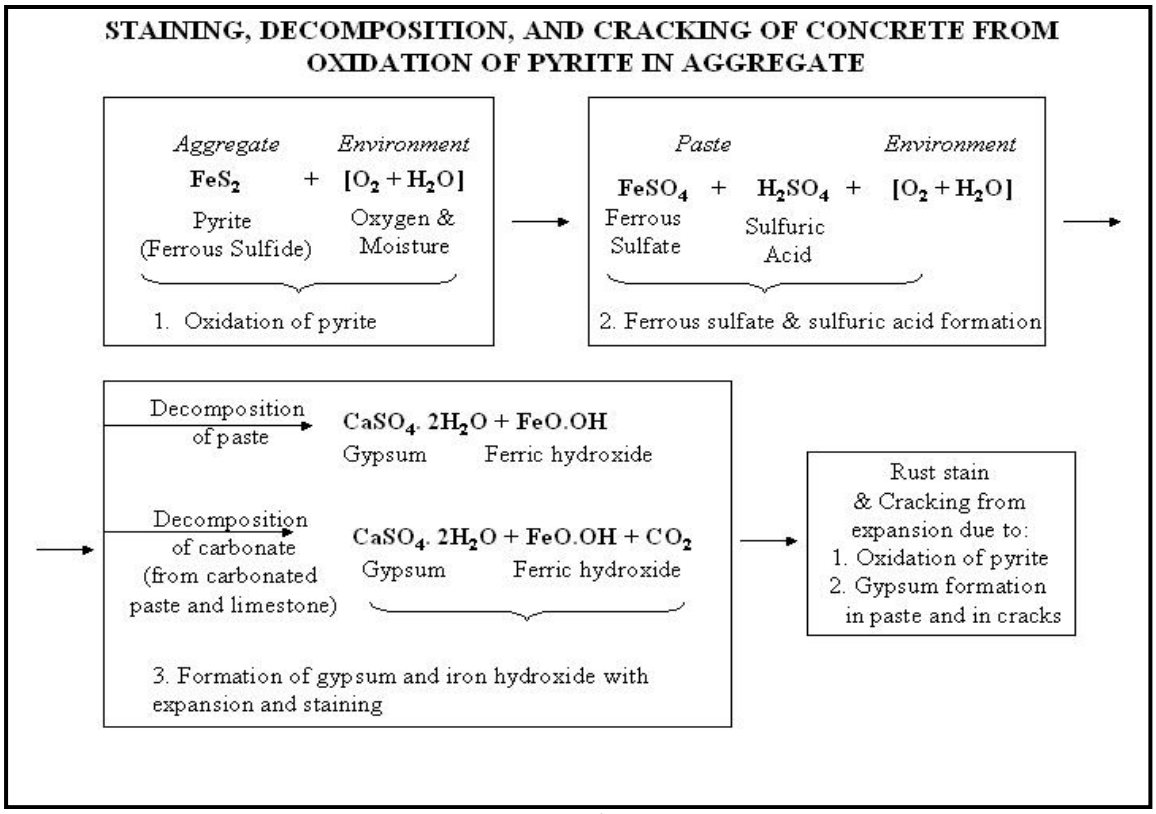

Figure 10 - Schematic diagram showing mechanism of concrete deterioration associated with oxidation of pyrite inclusions in coarse aggregate in concrete.

CASE STUDY II: CONCRETE DETERIORATION IN A CHIMNEY ENVIRONMENT

Background – A pre-1950s chimney, having concrete and brick-masonry liners showed noticeable weathering, erosion, cracking, discoloration, and deterioration of the interior walls of the concrete liner. A $3^3/_4$ in. diameter, $5^1/_4$ in. long concrete core, drilled from the inner wall of the liner at an elevation of 89-ft was received for examination. The core was examined by petrography to determine: (a) the overall quality, condition, and composition of the concrete in the liner; (b) evidence of any physical or chemical deterioration of concrete; and (c) the depth of visible surface deterioration of the liner wall inside the concrete.

Concrete – The concrete is non-air-entrained and made using: (a) natural siliceous gravel coarse aggregate having a nominal maximum size of 1 in. and containing granite, quartzite, schist, gneiss, sandstone, and chert; (b) natural siliceous sand fine aggregate having a nominal maximum size of $^3/_8$ in. and containing strained and unstrained quartz, quartzite, feldspar, granite, schist, ferruginous rocks, sandstone, siltstone, chert, and mafic minerals; (c) a portland cement content estimated to be 5 to $5^1/_2$ bags per cubic yard; (d) a variably decomposed and discolored hardened cement paste having a water-cement ratio estimated to be 0.48 to 0.54 (estimation is from the least decomposed to undecomposed areas in the body); and; (e) an air content estimated to be less than one percent. The concrete is reasonably dense and well consolidated. There is a deficiency of finer and intermediate sizes of coarse aggregate; thus, the total aggregate grading is poor. Both coarse and fine aggregate particles are well distributed in the concrete. The strained quartz, quartzite, schist, and chert particles in coarse and fine aggregates show evidence of alkali-silica reactions described below, and therefore, were chemically unsound during their service in the concrete.

Surface Conditions – One end of the core, representing the outside wall of the liner, has a rough and weathered surface with cracks. The opposite end, representing the inside wall of liner (Figure 11), is a weathered and rough fractured surface on which are soft, white to light yellow colored decomposed areas of paste in the intervening areas between the aggregate particles.

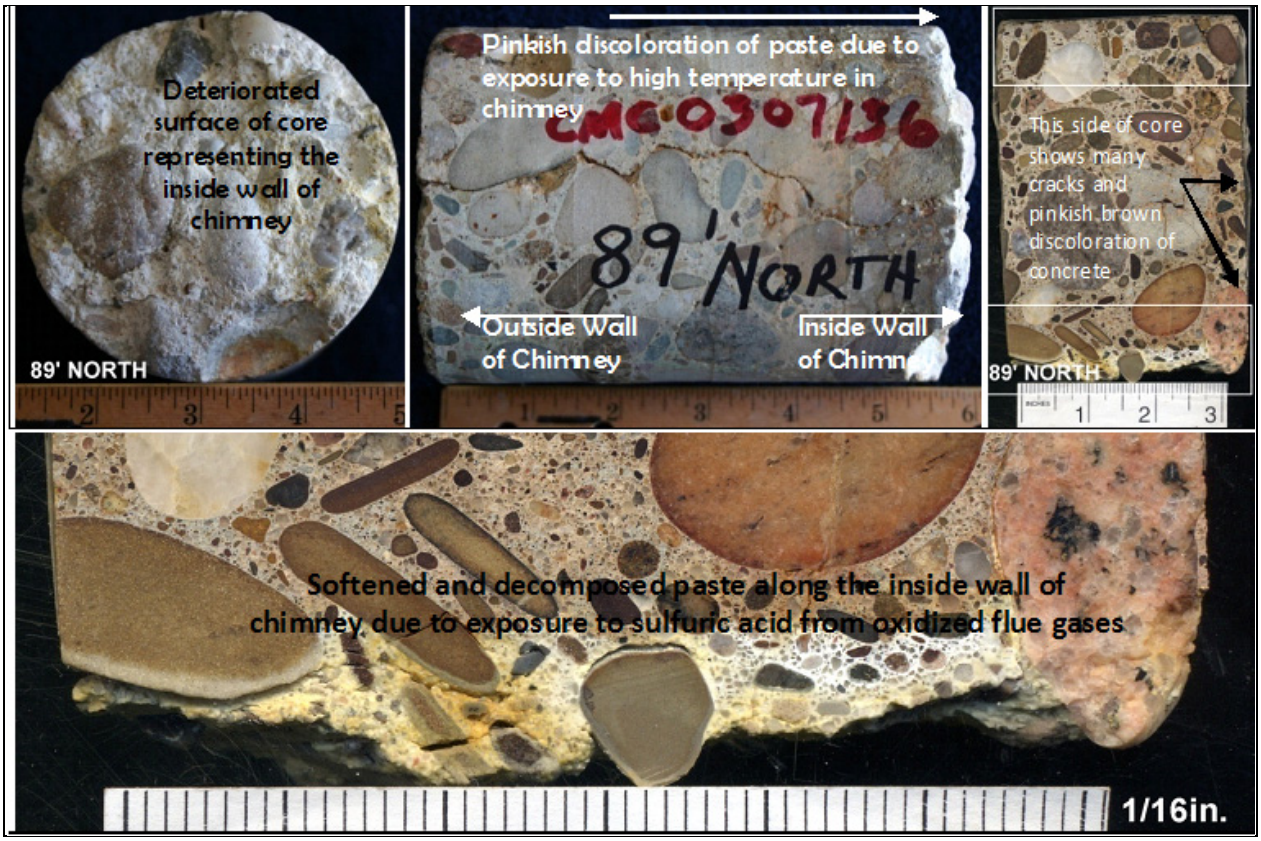

Figure 11 - The top left photo shows weathered end of a concrete core representing inside wall of a concrete liner in a chimney showing extensive deterioration and white deposits of gypsum. The top middle photo shows the entire core, which has a pinkish discoloration of paste at the inside end (marked with an arrow). The top right photo shows lapped cross section of the core showing cracking in concrete and pinkish discoloration at the bottom end (inside surface of liner). The bottom photo is an enlarged view of the bottom end of core showing thick deposits of gypsum, decomposition of paste, softening, and microcracking of decomposed paste.

Cracking – The core shows extensive cracking and fracturing, which have the following characteristics:

(a) The major (i.e., visible) cracks are longitudinal, i.e., oriented parallel to the long axis of the core (Figure 11);

(b) The cracks have transected and circumscribed the aggregate particles; a majority of these visible cracks have fractured some dense gneiss, quartzite and granite gravel coarse aggregates; many of these cracks have followed the aggregate-paste interfaces;

(c) The cracks are mostly concentrated at one side of the core (Figure 11), i.e., along one longitudinal edge of the core, and have extended to a distance of 1.5 in. from the edge – therefore, almost 50 percent (longitudinal half) of the core shows intense cracking and aggregate fracturing, whereas the adjacent half shows minimal cracking;

(d) Many visible cracks contain dark opaque deposits along the walls that are indicative of migration of smoke and burnt materials through the cracks (Figure 12); such precipitation of dark coat of materials along crack walls also indicate preexisting nature of the cracks; and

(e) Associated with macrocracks are many microcracks that are present in the paste, along the aggregate-paste interfaces and across the aggregate particles.

The nature and configuration of the cracks are indicative of their formation by a complex process involving: (a) alkali-aggregate reactions in concrete, and (b) differential thermal expansions of aggregates and paste as a result of exposure of concrete to high temperatures.

Thermal Discoloration of Concrete – On the longitudinal half of the core having intense cracking, concrete shows characteristic reddish to pinkish brown discoloration of paste, which is indicative of exposure to high temperatures of the chimney. The color of concrete changes from moderately dark reddish brown at the cracked edge through light brown in the central portion to medium gray at the opposite end. The discoloration is due to oxidation of iron-bearing phases in the aggregates at high temperatures. Based on the nature of the discolored paste the concrete is judged to have been exposed to a temperatures of 250 to 350°C.

On the fractured end of the core representing the inner wall of liner, paste shows soft, light yellow to white discoloration (Figure 12), which is due to formation of gypsum deposits on liner wall from decomposition of paste by sulfur-rich flue gases in the chimney.

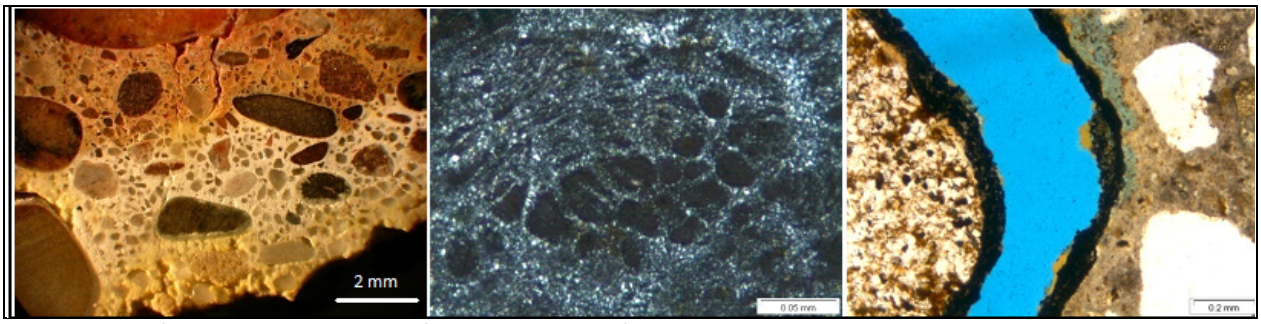

Figure 12 - Left = Photomicrograph of lapped section of core showing white gypsum deposits on the inside wall. Middle = Thin section photomicrograph (crossed polars) showing very fine crystals of gypsum in the decomposed paste. Right = Black deposits on the major vertical crack from chimney smoke.

Thermal Dehydration of Gypsum to Anhydrite – Although the present case study showed gypsum deposits on the corroded inside wall of concrete, in many case studies of concrete chimney deterioration, the author has detected not only gypsum but also anhydrite [$CaSO_4$], sometimes only anhydrite due to thermal dehydration of gypsum to anhydrite at high temperatures of chimney. The following x-ray diffraction pattern of another sample (Figure 13), from a different case study, which showed very similar white deposits on the corroded inside wall of a concrete chimney, as well as pinkish discoloration of paste, showed the presence of anhydrite but no gypsum.

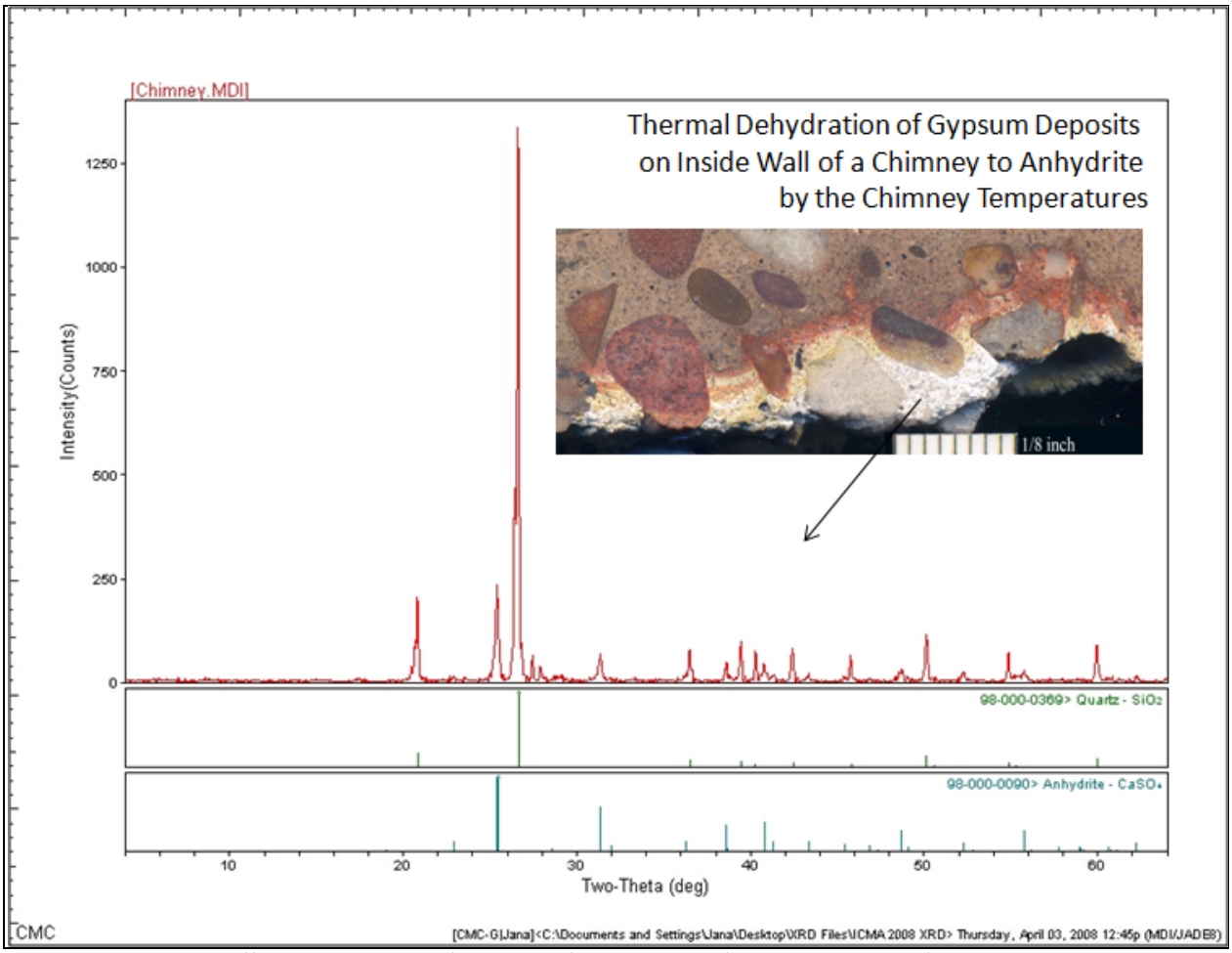

Figure 13 – X-ray diffraction pattern of white surficial deposits from inside wall of another chimney showing thermal dehydration of gypsum into anhydrite. The inset photo shows lapped cross section of a core from this chimney, where dark pinkish bands of discoloration of paste (from the high temperature exposure), above the white anhydrite deposits on the corroded inside wall is distinct.

Alkali-Silica Aggregate Reaction (ASR) – The coarse and fine aggregates contain many potentially alkali-silica reactive particles, such as strained quartz and quartzite, chert, strained granite, and schist. There are isolated, meager evidence of alkali-silica reaction in the concrete, which is diagnosed by dark reaction rims around some particles, microcracking associated with reactive particles many of which originated from the particles and extended into the neighboring paste (Figure 14), alkali-silica reaction gels inside the cracks (Figure 14), and evidence of burnt and dehydrated alkali-silica gel along a few microcracks. Cracking from alkali-silica reaction is distinguished from thermal cracking by their occurrence and association with reactive aggregates.

Reactive particles in both coarse and fine aggregate, high-alkali cement used in the concrete, intermittent exposure to moisture during service, and high temperatures of the chimney – all have contributed to the occurrence of alkali-silica reactions, and associated concrete deterioration. There is evidence of high temperature exposure of burnt and dehydrated reaction gel in the microcracks, which is indicative of the occurrence of such a reaction prior to a high temperature event, and possible multiple cyclic occurrences of reactions and high temperature exposures during the service life of chimney, where the effects of one process may have been masked by the other, or may have intensified the overall concrete deterioration.

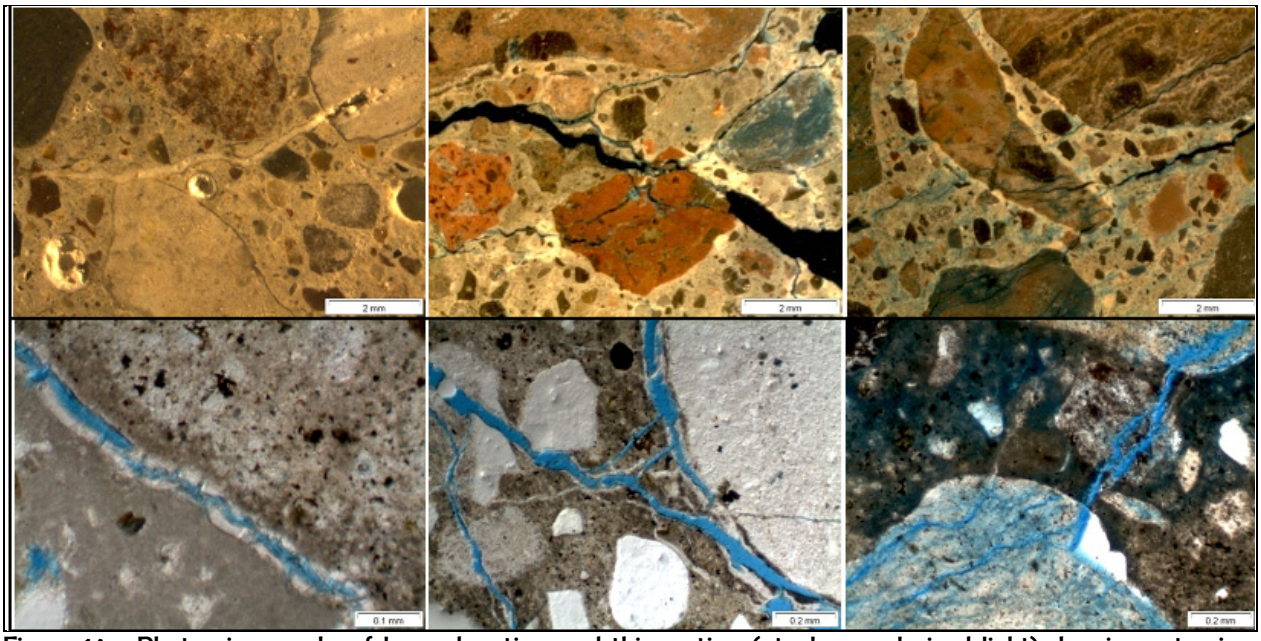

Figure 14 - Photomicrographs of lapped section and thin section (at plane polarized-light) showing extensive microcracking in aggregates and paste from alkali-silica aggregate reaction and white deposits of carbonated alkali-silica gel in many microcracks. Cracks in thin section photos are highlighted by blue dye mixed epoxy used to impregnate the sample.

Corrosion and Decomposition of Paste at the Inside Wall of Chimney Due to Acid Attack from Moist Flue Gases – At the rough, fractured, weathered end of the core (representing the interior wall of the chimney), paste shows white to light yellow discoloration, severe decomposition, carbonation, and formation of gypsum-rich layer as soft, discolored surface, which has extended inside to a distance of $^{1}/_{4}$ to $^{3}/_{8}$ in. (Figure 15). The portland cement hydration products in paste in this decomposed zone have essentially been altered to calcium sulfate composition (texturally very fine grained gypsum crystals, Figure 15), which is a common feature in many chimney concrete linings due to exposure to sulfur-rich chimney gases (i.e., SO_2). The decomposed paste, however, did not extend deep into the concrete, it is confined to within the maximum $^{3}/_{8}$ in. zone from the interior surface.

Flue gases usually do not attack concrete liner as long as they are dry. Intermittent exposure to moisture, however, generates acids, which causes acidic corrosion of concrete wall. Acidic corrosion of paste (and of carbonate aggregates, if present), formation of sulfate deposits from moist sulfur dioxide flue gas, carbonation from moist carbon dioxide gas, and the resultant overall softening and decomposition are the common features, which are usually controlled in modern chimneys by acid-resistant liners.

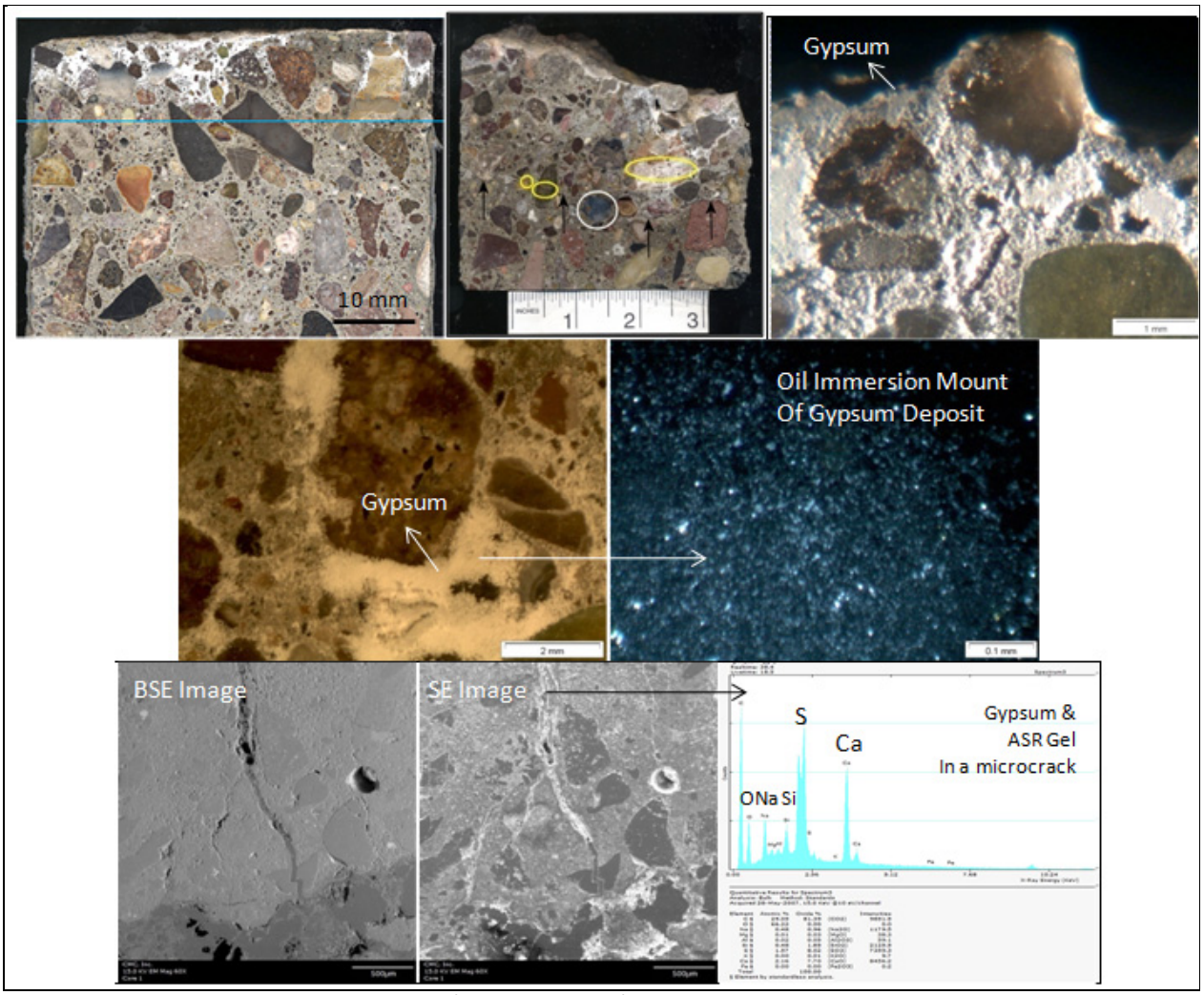

Figure 15 - Top = Lapped cross section of another core from a chimney environment showing white gypsum deposits on the surface (representing inside wall of concrete liner). The middle photo shows oil immersion mount of gypsum deposits. The bottom photos show backscatter and secondary electron images of a microcrack that is filled with gypsum and alkali-silica reaction gel. EDS spectrum of the deposits show Ca and S from gypsum and Na, Ca, Si from alkali-silica gel.

Evidence of High Temperature Exposures of Chimney in the Concrete Lining – The effects of high temperatures of chimney on concrete lining is evidenced from: (a) reddish brown discoloration of concrete along one longitudinal edge of the core; (b) intense cracking and microcracking of concrete in the discolored portion; (c) black smoke deposits inside the cracks; and (d) gypsum deposits on liner wall from flue gases, which in many cases dehydrate to anhydrite. The deleterious effects of high temperatures, i.e., cracking, have extended to almost half the longitudinal section of the core. The core, therefore, represents a portion of the concrete transitional between the exposures of high temperatures and associated distress and lesser temperatures with lesser amounts of distress.

Relative effects of ASR, Thermal Cracking, and Paste Decomposition by Flue Gases on Overall Concrete Deterioration – Due to intensive cracking and associated thermal attacks and alkali-aggregate reactions, the overall condition of the concrete in the core is judged to be poor. Gypsum deposits on inner wall from oxidized flue gases and associated paste decomposition, however, were confined to within $^{1}/_{4}$ to $^{3}/_{8}$ in., which is typical in many chimney environments, and did not contribute as much to the overall deterioration of concrete as by the other mentioned processes.

CASE STUDY III: CONCRETE DETERIORATION IN A SEWER ENVIRONMENT

Background – An approximately 30 to 40-year old concrete sewer line showed severe deterioration of the inside wall, mainly on the aerated portions of the line. Core samples, drilled from the submerged zone (i.e., portion continuously beneath the sewage effluent) and the transitional zone (i.e., portion mostly exposed to air and intermittently submerged during transportation of high volume sludge) were received for investigating depths of concrete damage in the submerged and transitional zones of the line.

Concrete – Concretes in the cores from the submerged and transitional zones are essentially similar in composition, as expected. The concrete is non-air-entrained and made using a mixture of siliceous gravel and pea gravel coarse aggregate having a nominal maximum size of $^{3}/_{4}$ in., natural siliceous sand fine aggregate having a nominal maximum size of $^{3}/_{8}$ in., a portland cement content estimated to be 6 to $6^{1}/_{2}$ bags per cubic yard; and a water-cement ratio estimated to be 0.44 to 0.48. The air content is estimated to be less than one percent. The concrete is very dense and well consolidated (see Figures 16 and 17). The aggregate particles are well graded, well distributed, and have been sound during their service in the concrete. Both coarse and fine aggregates are compositionally similar and made using siliceous gravels. Coarse aggregate contains quartzite, schist, gneiss, sandstone, chert, volcanic rocks, etc. Fine aggregate contains all the rock types of coarse aggregate plus quartz, feldspar, mafic minerals, ferruginous rocks, and siltstone. Despite the presence of many potentially alkali-silica reactive particles in both the coarse and fine aggregate, there is no evidence of such a reaction in the concrete. The paste in the body of concrete is very dense, hard, and contains residual and relict portland cement particles, and portland cement hydration products. There is no evidence of use of any pozzolanic or cementitious admixtures in the concrete.

Core from the Submerged Zone – Figure 16 shows detailed microstructure of the core from the submerged zone. The exposed surface has a typical smooth to weathered appearance with traces of sludge materials. Lapped cross section shows the dense, medium to dark gray, well consolidated nature of concrete and good grading and distribution of aggregates. The surface region shows light gray to light brown discoloration due to elemental migration and interactions with sludge materials.

Chemical Alteration at the Surface Region of Submerged Core – The top end of the core, representing the exposed inside surface of sewer channel in contact with the sludge shows a thin layer of discolored paste, which is approximately $^{1}/_{4}$ in. thick from the surface. The paste is light brown to cream-colored compared to the normal gray color of the paste in the body. At the very top of the concrete is a thin region of multiple compositional zoning consisting of (Figure 16): (a) a light reddish brown color, soft, leached, and carbonate paste, (b) a thin line of dark gray to black color film of sludge materials immediately beneath the reddish brown carbonated paste, (c) an inner zone of leached and carbonated paste situated immediately beneath the dark line, where paste lacks calcium hydroxide component of portland cement hydration, and shows some very fine, hair-sized microcracks oriented parallel to the exposed surface, (d) air voids within the leached and carbonated zone show secondary gypsum precipitation due to interactions with sewage effluents, and eventually, (e) the sound interior concrete. The entire thickness of the discolored and altered zones (Items 'a,' 'b,' and 'c') is very thin, approximately $^{1}/_{4}$ in. in maximum thickness, which is indicative of limited interactions of sewage effluents with the concrete paste. The severity of such an interaction is low, mainly due to the continuously submerged location of the core and the dense, good nature of the concrete. The main body of the concrete beyond the $^{1}/_{4}$ in. surface zone of chemical alteration is sound and judged to be of good quality. The siliceous nature has prevented chemical alteration or decomposition of the aggregate particles by the sewage effluents.

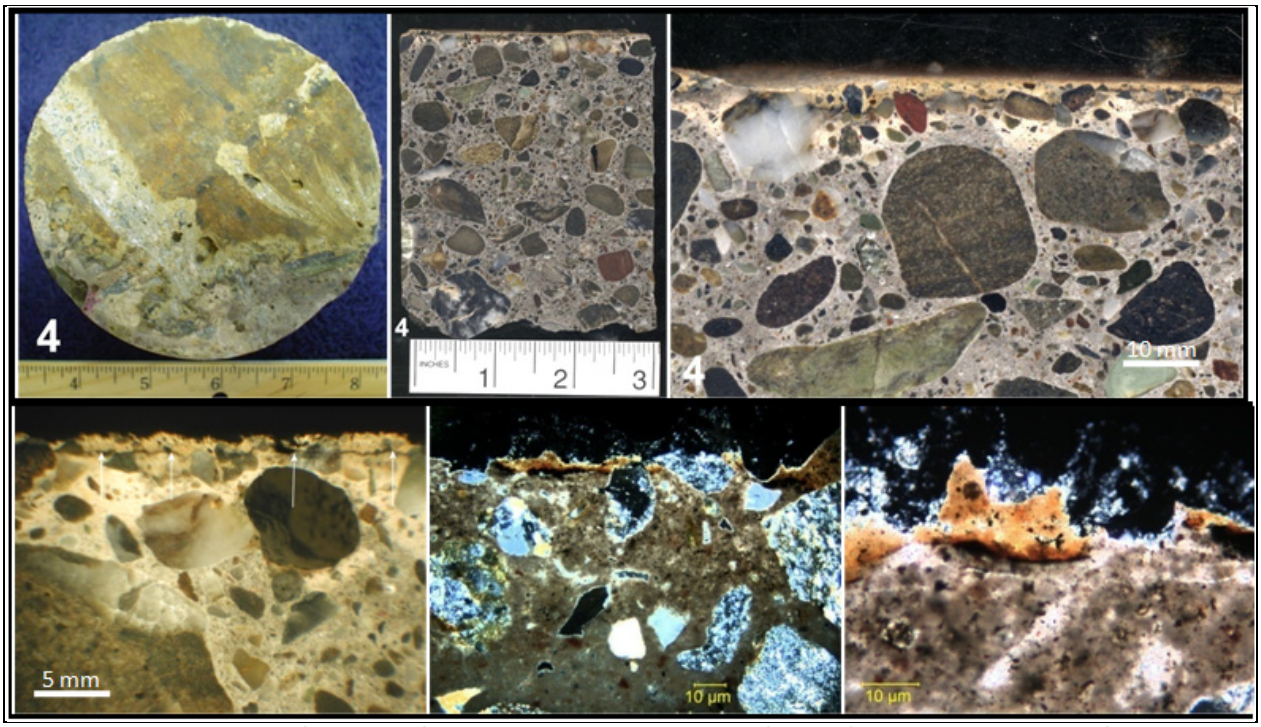

Figure 16 - Photographs of the core from the submerged portion of the influent channel. Top left = Core end representing inside wall of the channel. Top middle = Lapped cross section of the core. Top right = Enlarged view of the lapped cross section from the top showing white gypsum deposits on the surface. Bottom left = Lapped cross section showing sludge deposits on carbonated and decomposed paste and white gypsum deposits on the decomposed concrete. Bottom middle = Thin section photomicrograph of the inside wall showing reddish brown ferruginous deposits in sludge on the surface, carbonated and decomposed paste, and white gypsum deposits in the voids. Bottom right = Thin section photomicrograph showing carbonated paste and reddish brown ferruginous deposits from the sludge.

Core from the Transitional Zone – Figures 17, 18, and 19 show the core from the transitional zone, and the detailed microstructure of concrete deterioration at the exposed surface region, which is mostly confined to within the top $^{1}/_{4}$ in. (most deterioration), and shows its minor effects down to a maximum depth of $1^{3}/_{4}$ in.

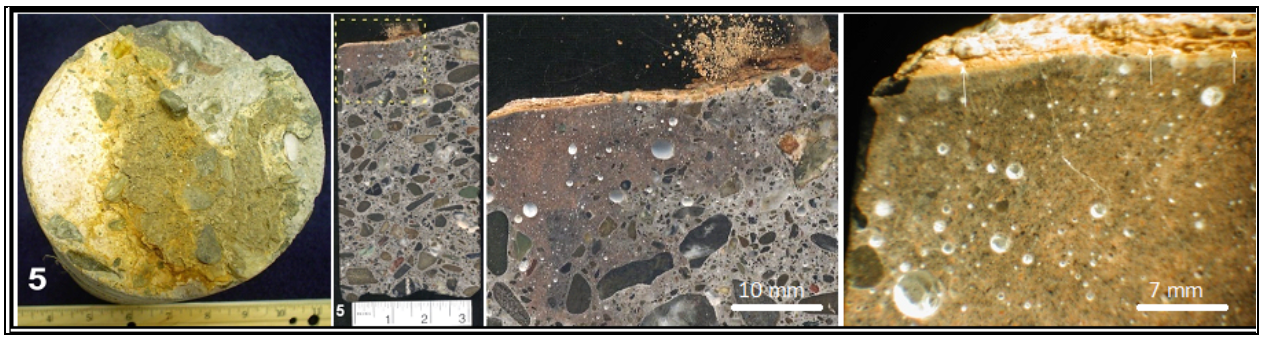

Figure 17 - Photographs of the core from the transitional zone of the influent channel. Left = Core end representing inside wall of the channel and showing severe discoloration, corrosion, and alteration of concrete. Next Right = Lapped cross section of the core showing overall dense, well-consolidated nature of concrete and reddish brown discoloration and softening of paste with a thin zone of microcracking at the surface region (boxed). Next Right = Enlarged view of the boxed area in the lapped cross section showing discoloration and alteration of concrete at the surface region only, and the presence of white secondary deposits in air voids to a depth of 10 to 20 mm. The rightmost photo shows microcracking at the surface region (within the top 5 to 7 mm), which are shown in detail in Figure 18.

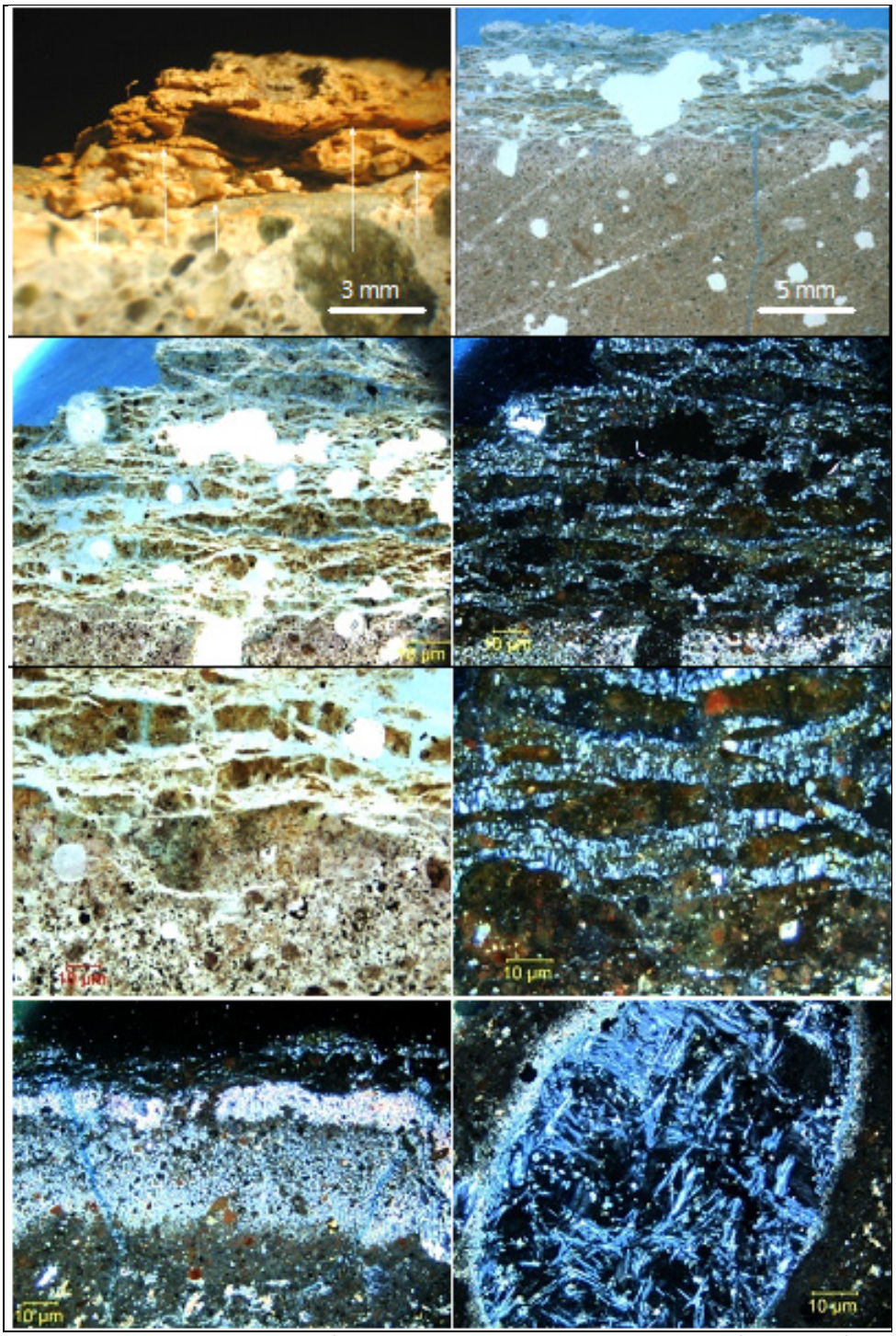

Figure 18 - Photomicrographs of lapped cross section and thin section of the core from the transitional zone of sewer pipe showing the exposed surface region. Notice severe deterioration, extensive cracking and microcracking, carbonation of paste, leaching of paste beyond the carbonated zone, and extensive gypsum and altered paste deposits filling the cracks (gypsum crystals oriented perpendicular to the crack walls) and voids in the altered zone at the surface, which is present within the top 10 mm of the exposed corroded surface. All photos, except the top left one, are of thin sections taken by using a petrographic microscope, at magnifications of 40 to 100x.

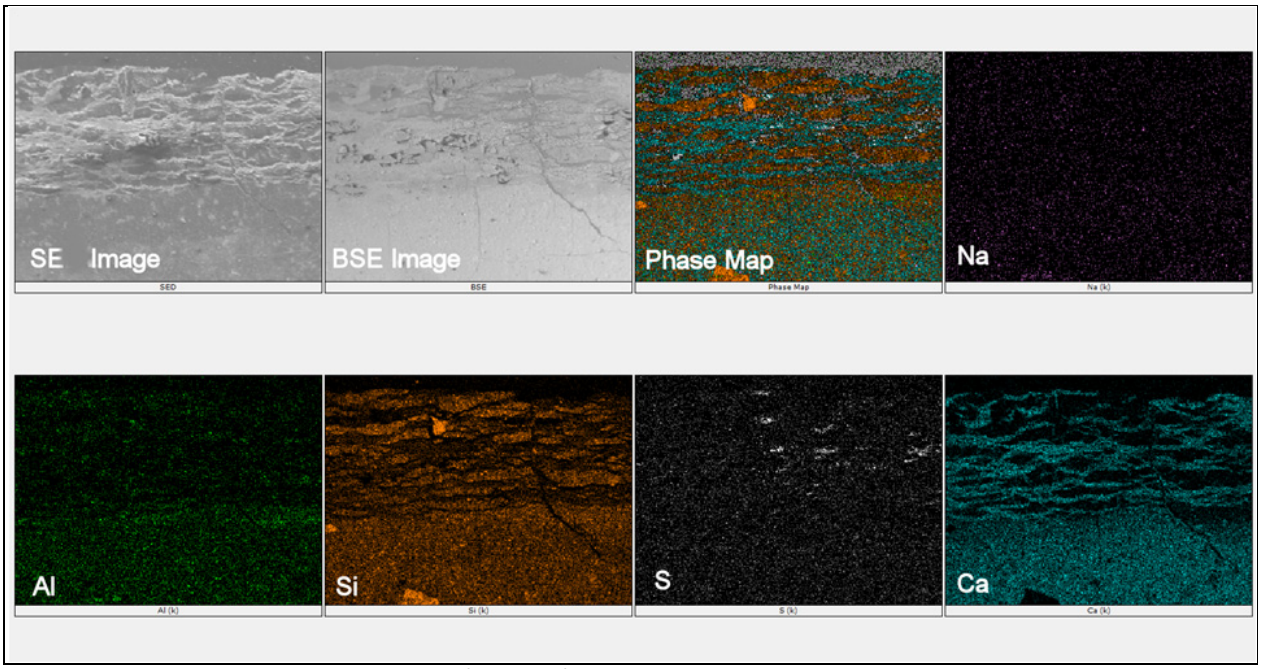

Figure 19 – X-ray elemental mapping of the surface region showing altered paste and disseminated gypsum deposits in the surface-parallel microcracks.

Chemical Alteration at the Exposed Surface Region of the Core from the Transitional Zone

- The top end of the core represents the intermittently exposed (transitional zone) inside surface of the channel wall where the concrete shows staining, severe deterioration, alteration of the paste, surface-parallel microcracking and deposition of the products of alteration of the concrete by the sewage effluents (Figure 18).

On the exposed surface, one-half portion of the surface has a white and light yellowish brown discolored and soft powdery nature due to precipitation of gypsum on the surface. Immediately beneath the white gypsum layer is a dark reddish brown oxidized layer of chemically altered and decomposed paste, where the concrete surface shows severe microcracking and the presence of numerous thin microcracks oriented parallel to the surface; many of these microcracks are filled with decalcified calcium silicate hydrate of paste and secondary deposits of gypsum (see Figures 18 and 19), and the paste is severely leached (lacking calcium hydroxide component of cement hydration), altered, and dark brown stained. The microcracked surface region and the white gypsum film together are approximately $^{1}/_{16}$ in. thick. Immediately beneath the microcracked and distressed surface, paste is denser and of better quality but has a dark purple/brown coloration, which has extended to a depth (distance) of $1^{3}/_{4}$ in. from the deteriorated surface. Within this discolored interior concrete are air voids that are lined or filled with white secondary gypsum and ettringite deposits, due to the interaction of cement hydration products with the sewage effluents. The staining, leaching, discoloration, surface microcracking, gypsum precipitation of the surface as white film, gypsum precipitation in the air voids in the interior concrete down to a depth of $1^{3}/_{4}$ in., staining of the interior paste down to $1^{3}/_{4}$ in. – all these features are present on one longitudinal half of the core, which is judged to represent the intermittently aerated portion of the wall. The other longitudinal half of the core has a fresh fractured surface at the top and no severe staining, leaching, microcracking, or discoloration of the paste. In the altered side of the core, the surface deterioration is confined to within $^{1}/_{16}$ to $^{1}/_{8}$ in. of the stained surface and the depth of discoloration of paste with gypsum/ettringite deposits in the air voids has extended to a maximum distance of $1^{3}/_{4}$ in. Concrete beyond that region is sound and of good quality.

In Summary: There is clear evidence of interaction of sewage effluents with the concrete surface at the transitional zone of the inside wall of the channel, where gypsum formation at the surface, reddish brown staining, discoloration of paste, microcracking at the top $^{1}/_{16}$ in., and staining of paste down to a distance of $1^{3}/_{4}$ in. are clear. Despite such evidence of surface deterioration, microcracking, staining, leaching, and gypsum precipitation, which is not uncommon in the aerated portion of a concrete sewage pipe, the distance of such deterioration is still minimal (severe deterioration up to $^{1}/_{16}$ to $^{1}/_{8}$ in. and evidence of staining down to a distance of $1^{3}/_{4}$ in.). The concrete in the body beyond the deteriorated surface region in the aerated portion of the channel is good and in sound condition. It is the dense nature of the concrete, which is responsible for the good condition of concrete in the interior.

Gypsum formation in the aerated portion of the inside wall of the channel is the result of oxidation of sewage gas (hydrogen sulfide) to sulfuric acid by the aerobic, sulfur-oxidizing bacteria that colonizes in the aerated portion of the inner wall of the channel [1, 2]. A thin film of moisture in the aerated inside wall of the channel helps colonization of sulfur-oxidizing bacteria (e.g., thiobacillus), which oxidizes hydrogen sulfide gas (that emits out of the sewage effluents) into sulfuric acid in the moisture film of the wall. Sulfuric acid, generated from such bacterial oxidation then causes not only acid attack to the concrete surface but also sulfate attack. Reaction of sulfuric acid with the calcium hydroxide component of portland cement hydration in the concrete paste causes leaching of calcium hydroxide from the paste from the surface region by the acidic action and formation of gypsum. Carbonate aggregates, if present, can also be decomposed by sulfuric acid (which is not the case here due to the presence of siliceous aggregates). Gypsum formation at the surface region causes formation of surface-parallel microcracks. Light yellowish brown and white discolorations are the results of interaction of sulfur-bearing components in the sewage with the concrete. Leaching, gypsum formation, microcracking, staining, deterioration occurs from the surface and progressively advances into the concrete. The depth or extension of such alteration/deterioration depends among other things (e.g., pH, temperature, type of bacterial growth, sewage flow) on the quality and condition of the concrete. Concrete in the present core is judged to be of good quality to confine the chemical alteration essentially at the surface region (to a maximum distance of $1^{3}/_{4}$ in.). The surface of the core itself, however, is spalled and severely altered, which prevents determination of the actual depth/distance of deterioration.

SIMILARITIES OF CONCRETE MICROSTRUCUTRES BETWEEN THREE ENVIRONMENTS

All three case studies, from widely different environments, show similar decomposition of concrete at the surface exposed to the environment, e.g., spalling or popout, microcracking, softening of paste, alterations, gypsum formation, carbonation, loss of mass and strength, etc. (Figure 20). In all cases, sulfuric acid, generated either by moisture-induced oxidation of pyrite, or from oxidized chimney flue gases, or from oxidized hydrogen sulfide gases in the sewer environment has caused the decomposition. It is the good, dense, and near-impermeable nature of concrete to sulfuric acid that has restricted such attacks to essentially near the exposed surface regions of concretes. Unlike the sewer environment, where aerobic bacterial-induced acid attack is the common and primary mechanism of concrete deterioration, in the cases of pyrite oxidation and chimney environment, however, acidic corrosion is a secondary mechanism, which occurs in association with staining/popout and thermal attacks, respectively.

Similar microstructural features of concrete deterioration (e.g., surface-parallel microcracking, exfoliation, softening of paste, gypsum formation, loss of mass and strength) are common in the classical external sulfate attacks of concrete exposed to a sulfate-rich soil. Author's other cases related to deterioration of concrete septic tanks and waste water treatment tanks that generate hydrogen sulfide gases similar to the sewer pipe environment shown here also show similar features of white gypsum deposits on the exposed corroded surface, mushy appearance of concrete at the cases of severe

alterations, microcracking, and other related deterioration. The nature of the sulfuric acid and sulfate attacks to concrete are similar, irrespective of the environment in which it occurs.

In all these cases of acid and sulfate attacks in concrete, a detailed petrographic examination (optical and scanning electron microscopy, x-ray diffraction) and associated chemical analysis can determine the depth or distance of such attacks, provide an overall assessment of the condition of concrete at and beyond the deteriorated zones, and evaluate future durability in such environments.

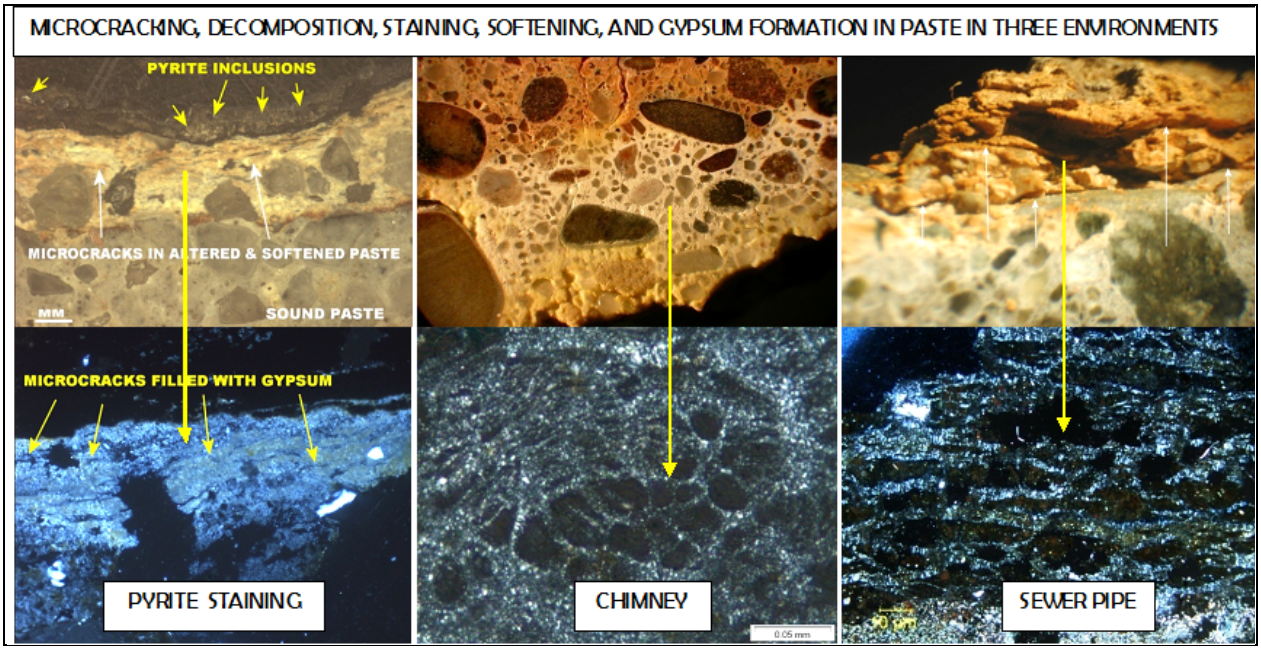

Figure 20 - Microstructural similarities of concrete deterioration in three environments shown by photomicrographs of lapped cross sections (top row photos) and corresponding thin sections (bottom row) of samples. In all cases, concrete show microcracking, softening and decomposition of paste, and gypsum formation – all due to the exposures to sulfuric acid and associated sulfate attacks in the paste.

ACKNOWLEDGMENTS

From the preparation of the original reports of case studies presented here, to selection and compilation of studies in this paper, review, editing, photo arrangements, and deign and formatting of layouts, Jennifer Lee Hall has been a constant help, without whom the paper would not have been possible. Mitzi Casper meticulously prepared the samples for laboratory studies, took photomicrographs, described the samples as received, and did preliminary petrographic examinations. Heartfelt thanks go to all my industry clients, who kept faith on me, send samples for these interesting projects, and helped me understand the concrete deterioration processes.

REFERENCES

1. St. John, D.A., Poole, A.W., and Sims, I., Concrete Petrography – A Handbook of Investigative Techniques, Arnold, 1998, 474p.
2. Jana, D., and Lewis, R.A., Acid Attack in a Concrete Sewer Pipe – A Petrographic and Chemical Investigation, Proceedings of the 27th Conference on Cement Microscopy, ICMA, 2005.